STM JOURNALS

Journal of
Polymer & Composites

ISSN: 2321-2810 (Online)
ISSN: 2321-8525 (Print)
Volume 14, Special Issue 3, 2026
DOI (Journal): 10.37591/JoPC

https://journals.stmjournals.com/jopc

Research JoPC

Valorization of Human and Cattle Dental Waste into Functional Composite Biomaterials: A Detailed Comparative Analysis

Subhasis Nath[1], Sourav Debnath[2], Soumya Mukherjee[3], Sujan Krishna Samanta[4,*]

Abstract

This study investigates the conversion of human and cattle (goat and cow) teeth into bioactive hydroxyapatite-based composites and presents a detailed comparative evaluation of these biogenic materials with laboratory-synthesised (synthetic) hydroxyapatite (HAp). In this work, hydroxyapatite was extracted from human and bovine teeth through controlled calcination and milling, while synthetic HAp was prepared using a standard wet chemical precipitation route. All materials were subsequently sintered at 900 °C and fabricated into pellets for physical and biological analysis. X-ray diffraction (XRD) analysis confirmed that all samples—synthetic and biogenic—possessed crystalline structures consistent with stoichiometric hexagonal hydroxyapatite. FTIR spectra revealed characteristic phosphate, hydroxyl, and carbonate functional groups, with biogenic samples showing slightly higher carbonate substitution. Physical characterization demonstrated comparable hardness, shrinkage behaviour, densification, and porosity among the samples, with only minor variations attributable to natural ionic substitutions present in biological apatite. SEM analysis revealed interconnected porous microstructures favourable for osteoconduction, while pore-size distribution remained consistent across all groups. A strong negative correlation between porosity and hardness (r = –0.996) affirmed the influence of pore architecture on mechanical properties. Biological evaluations validated the suitability of the materials for biomedical use. MTT cytotoxicity assays demonstrated high cell viability (>95%) for all samples, indicating excellent cytocompatibility. Haemolysis percentages remained below the ASTM threshold of 5%, confirming hemocompatibility. Simulated Body Fluid (SBF) immersion studies showed enhanced apatite formation in biogenic HAp compared to synthetic HAp, highlighting superior bioactivity due to natural trace ions and surface reactivity. The findings establish human and cattle teeth as promising, sustainable resources for producing high-quality hydroxyapatite suitable for applications in bone regeneration, implant coatings, and other biomedical domains.

***Author for Correspondence**
Sujan Krishna Samanta

[1]Principal, Department of Mechanical Engineering, Central Tool Room and Training Center, Kolkata, West Bengal, India
[2]Assistant Professor, Department of Electrical Engineering, Brainware University, Kolkata, West Bengal, India
[3]Assistant Professor, Department of Metallurgical Engineering, Kazi Nazrul University, Asansol, West Bengal, India
[4]Associate Professor, Department of Biomedical Engineering, Netaji Subhash Engineering College, Kolkata, West Bengal, India

Received Date: March 17, 2026
Accepted Date: March 25, 2026
Published Date: May 07, 2026

Citation: Subhasis Nath, Sourav Debnath, Soumya Mukherjee, Sujan Krishna Samanta. Valorization of Human and Cattle Dental Waste into Functional Composite Biomaterials: A Detailed Comparative Analysis. Journal of Polymer & Composites. 2026; 14(Special Issue 3): S340–S354p.

Keywords: Biomedical waste, haemocompatibility, teeth, cattle, bioactive biomaterials

INTRODUCTION

The increasing amount of different categories of waste [1] has become a critical concern worldwide. Many natural materials [2, 3] and diverse waste products [4] were investigated by different researchers for multiple applications [5]. Different modifications [6] have been made to these wastes to improve their performance and make them suitable for practical and value-added purposes. One big concern today is that the daily generation of biomedical waste from hospitals, clinics, and slaughterhouses presents serious environmental

challenges, particularly when waste management practices are inefficient. Among these wastes, discarded teeth represent a unique concern [7]. Biomedical waste is not only an ecological hazard but also a potential source of pathogen contamination, making effective management and reduction strategies essential. Interestingly, teeth—largely composed of calcium-based compounds such as hydroxyapatite ($Ca_{10}(PO_4)_6(OH)_2$)—offer potential value as raw material for bioactive ceramic-based composite substances [8].

Since Professor Hideki Aoki first reported the bioactive and bioresorbable properties of hydroxyapatite in 1972, extensive research has explored its biomedical applications [9–12]. Various synthesis techniques, including hydrothermal processing [13, 14] chemical precipitation [15], sol-gel methods [16], multiple emulsions [17, 18], biomimetic deposition, and electrodeposition, [19] have been employed to produce hydroxyapatite. In addition, natural biological sources such as shells and bones [20, 21] have been investigated as sustainable alternatives for hydroxyapatite production. The use of low-cost natural sources for ion-doped hydroxyapatite (HA) has attracted considerable attention. Materials such as mammalian and fish bones [22, 23], eggshells [24, 25], corals [26] animal bones [27], seashells, and even certain plants [28] provide abundant calcium and phosphate, while also offering opportunities for ion doping to enhance HAp properties. These sources represent a cost-effective and environmentally sustainable approach to HAp synthesis, with applications spanning biomedicine, tissue engineering, and environmental remediation.

Efficient extraction and processing of such materials can drive innovation in material science, improving the accessibility of HAp for practical use. For instance, Ruksudjarit et al. [29] successfully synthesized nanocrystalline HAp powder from bovine bone using vibro-milling, while Jaber et al[27] demonstrated HAp production from Camelus bone, highlighting the versatility of bone-derived HAp. Despite significant progress in synthetic methods and bone-based sources, teeth—though a primary natural reservoir of hydroxyapatite—remain underexplored. As a form of biomedical waste, discarded teeth present a sustainable opportunity to produce nanocrystalline HAp, while simultaneously reducing environmental pollution and providing a viable material for bone graft applications. This study, therefore, aims to develop bioactive biomaterials derived from waste teeth collected from diverse sources, with a focus on comparing the properties of materials synthesized from human and bovine teeth.

MATERIALS & METHODS

Collection and Preparation of Biological Composite Samples

Human teeth extracted for clinical or surgical purposes were collected from hospitals and dental clinics, while cattle teeth were sourced from local slaughterhouses. All samples were initially rinsed thoroughly under running tap water to remove surface debris. Subsequently, the teeth were cleaned with boiled water and treated with analytical-grade ethyl alcohol (LR grade, >99% assay, MERCK India) to eliminate residual organic matter, including fats and proteins.

The cleaned teeth were then subjected to calcination in a high-temperature furnace at 800 °C for 2.5 hours to remove residual organic components and convert the mineral phase into a crystalline hydroxyapatite-based composite. After calcination, the material was ground using a ball mill for 2 hours to obtain a fine powder. The ground material was further processed using a sequential mechanical sieve shaker, and the finest fraction was collected as biogenic hydroxyapatite (HAp).

Synthesis of Laboratory-Grade Hydroxyapatite

Synthetic hydroxyapatite was produced using a standard wet-chemical precipitation method [30]. In this procedure, ortho-phosphoric acid (H_3PO_4) was slowly added to a stirred suspension of calcium hydroxide [$Ca(OH)_2$], allowing controlled nucleation and precipitation of hydroxyapatite. The reaction was carried out at a temperature range of 75–80 °C, and the pH of the mixture was maintained between 11 and 12, which is essential for promoting hydroxyapatite crystal formation. Continuous stirring ensured uniform mixing and particle growth throughout the reaction.

Fabrication and Sintering of Hydroxyapatite based composite Samples

The hydroxyapatite powders were compacted into cylindrical pellets using a hydraulic press (PEECO Pvt. Ltd., Kolkata, India). Uniaxial compression was performed in a steel die with an internal diameter of 8 mm, applying a load corresponding to 150 MPa for a duration of 3 minutes[31]. The green ceramic bodies obtained after compaction were assessed for green density based on their mass-to-volume (m/v) ratio.

Following initial characterization, the green pellets were sintered in a muffle furnace at 900 °C for 2 hours, with a constant heating rate of 6 °C/min. The sintering process facilitated densification and enhanced crystalline development within the material. The sintered specimens were subsequently examined using Scanning Electron Microscopy (SEM) to evaluate their surface morphology and microstructural features.

Pore Size Analysis

The pore dimensions of the synthetic hydroxyapatite and the biogenic HAp samples were evaluated by examining fractured surfaces of the sintered pellets. Each pellet was manually broken to expose the internal microstructure, and the fractured cross-sections were observed under a Scanning Electron Microscope (SEM). Pore diameters were measured using Perfect Screen Ruler software. For each sample type, five SEM micrographs were captured at comparable magnifications, and the pore sizes obtained from these images were averaged to obtain a representative pore dimension for reporting.

Phase Composition Analysis

The phase composition, crystallinity, and lattice parameters of the synthesized hydroxyapatite powders were evaluated using X-ray diffraction (XRD) analysis. All samples were indexed assuming a hexagonal crystal system, consistent with the structure of stoichiometric hydroxyapatite. The lattice constants were calculated using the major diffraction peaks and applying the standard interplanar spacing relation for a hexagonal lattice:

$$\frac{1}{d^2} = \frac{4}{3}\left(\frac{h^2 + hk + k^2}{a^2}\right) + \frac{l^2}{c^2}$$

where Miller indices of a plane are h,k,l. $\lambda = 2d\text{Sin}\theta$, where d is taken as the distance between next adjacent planes in the conventional set of Miller indices (h k l) and $\lambda = 1.54056$. Fourier-transform infrared spectroscopy (FTIR) was also conducted to confirm the presence of functional groups on the powdered samples.

Hardness Study

The mechanical integrity of porous biomaterials is critical, as the implanted structure must possess adequate strength to withstand physiological tissue pressures. In this study, the hardness of the sintered samples was evaluated using a Vickers hardness testing machine (VM-50, Instr. &Engg., India). A diamond indenter was employed, having the geometry of a square-based pyramid with an angle of 136° between opposite faces (equivalent to 22° between the indenter face and the sample surface).

The Vickers hardness value (HV) was determined using the standard relation:

$$HV = \frac{F}{A}$$

where F is the applied load, A is the surface area of the indentation, and d represents the average diagonal length of the imprint produced by the indenter. The hardness values are expressed in GPa.

Bioresorption Analysis

A bioresorption study was conducted to evaluate the dissolution behaviour of the sintered

hydroxyapatite samples in a biologically relevant environment. Simulated Body Fluid (SBF), prepared according to the Kokubo protocol [32] was used as the test medium and maintained at a physiological pH of 7.4.

The sintered pellets were fully immersed in the SBF solution and kept under controlled laboratory conditions (37°C). To ensure ionic stability and prevent saturation effects, the SBF solution was replaced every three days. The experiment was continued for a total duration of one month to allow sufficient time for dissolution and possible reprecipitation processes. After completion of the immersion period, the surfaces of the samples were examined using Scanning Electron Microscopy (SEM) to analyze apatite layer formation and to assess the extent of bioresorption and mineral deposition on the pellet surfaces.

Cytotoxicity Assessment (MTT Assay)

The cytotoxicity of the synthesized synthetic HAp and biogenic HAp samples was evaluated using the MTT assay performed on Peripheral Blood Mononuclear Cells (PBMCs) obtained from NCCS, Pune. Cells were seeded into 24-well plates at a density of 5×10^4 cells/cm² and allowed to adhere. The cells were then treated separately with each of the prepared HAp samples and incubated for 24 hours.

Following incubation, MTT solution was added to each well, gently shaken for 15 minutes, and further incubated for 4 hours to allow the formation of formazan crystals. After removing the supernatant, DMSO was added to dissolve the crystals, yielding a purple solution whose colour intensity corresponds to the number of viable cells. The absorbance of each well was measured at 545 nm using a microplate reader. The assay was performed in triplicate, and the average values were used for analysis.

The percentage cell viability was calculated based on the optical density relative to the untreated control.

The OD of the untreated control group is considered 100% viability, and all other OD readings are compared to it. Percentage cell viability is calculated using:

$$\text{Cell Viability (\%)} = \frac{OD_{\text{sample}}}{OD_{\text{control}}} \times 100$$

Haemolysis Study

An in vitro haemocompatibility assessment was performed using human blood following the guidelines provided in ASTM standards [33]. Fresh human blood was collected and mixed with 3.8% sodium citrate solution (as an anticoagulant) in a 10:1 ratio. To further dilute the anticoagulated blood, normal saline was added in a 4:5 ratio.

For the test group, 10 mL of normal saline was placed in test tubes, and the HAp sample pellets were immersed and incubated at 37°C for 30 minutes. Subsequently, 0.2 mL of the diluted blood was added to each test tube and incubated again at 37°C for 1 hour. Positive control was prepared by taking 10 mL of 0.1% sodium carbonate solution ,0.2 mL diluted blood and incubated at 37°C for 1 hour.

Negative control was prepared by10 mL normal saline, 0.2 mL diluted blood and incubated under identical conditions. After incubation, all tubes were centrifuged at 500 g for 5 minutes, and the supernatant was collected to measure the optical density (OD) at 545 nm using a UV–Vis spectrophotometer (Elico India, SL-177). The percentage haemolysis was calculated by using the standard formula:

$$\text{Haemolysis(\%)} = \frac{\text{OD}_{\text{sample}} - \text{OD}_{\text{negative control}}}{\text{OD}_{\text{positive control}} - \text{OD}_{\text{negative control}}} \times 100$$

Statistical Analysis

For each experimental condition, measurements were collected in triplicate (n = 3), and the data were expressed as mean ± standard deviation (SD).

RESULTS & DISCUSSION

Physical Properties

The physical characteristics of porous specimens (sintered at 900°C) of dimension (8 × 6 mm^2) are presented below in Table 1.

Table 1. The data of different physical properties.

Sample	Hardness (GPa)	Green density (g/cc)	Sintered density(g/cc)	Apparent porosity (%)
Synthetic HAp	3.85±0.04	2.504±0.020736	2.91±0.03	20.74±2.09
Cow Teeth HAp	3.79±0.15	2.628±0.013038	2.86±0.07	23.53±2.45
Goat Teeth HAp	3.76±0.11	2.596±0.011402	2.83±0.13	25.29±3.74
Human Teeth HAp	3.66±0.23	2.602±0.008367	2.81±0.02	28.97±3.02

The experimental data indicate that the hardness values and sintered density of hydroxyapatite across various tooth specimens are relatively consistent and exhibit values closely aligning with the hardness of synthetic HAp. This observation underscores a significant similarity in hardness properties between the natural and synthetic forms of HAp. This value closely aligns with the findings reported by Hoepfner and Case [34], P. Bhattacharjee et al., [35], and Acharjee et al. [36], thereby reinforcing the consistency and reliability of the observed hardness values in comparison to previous studies.

Across all groups, the synthetic HAp exhibits the highest hardness and sintered density, along with the lowest apparent porosity (Figure 1). Conversely, human-teeth HAp shows the lowest hardness, lowest sintered density, and highest porosity**.**

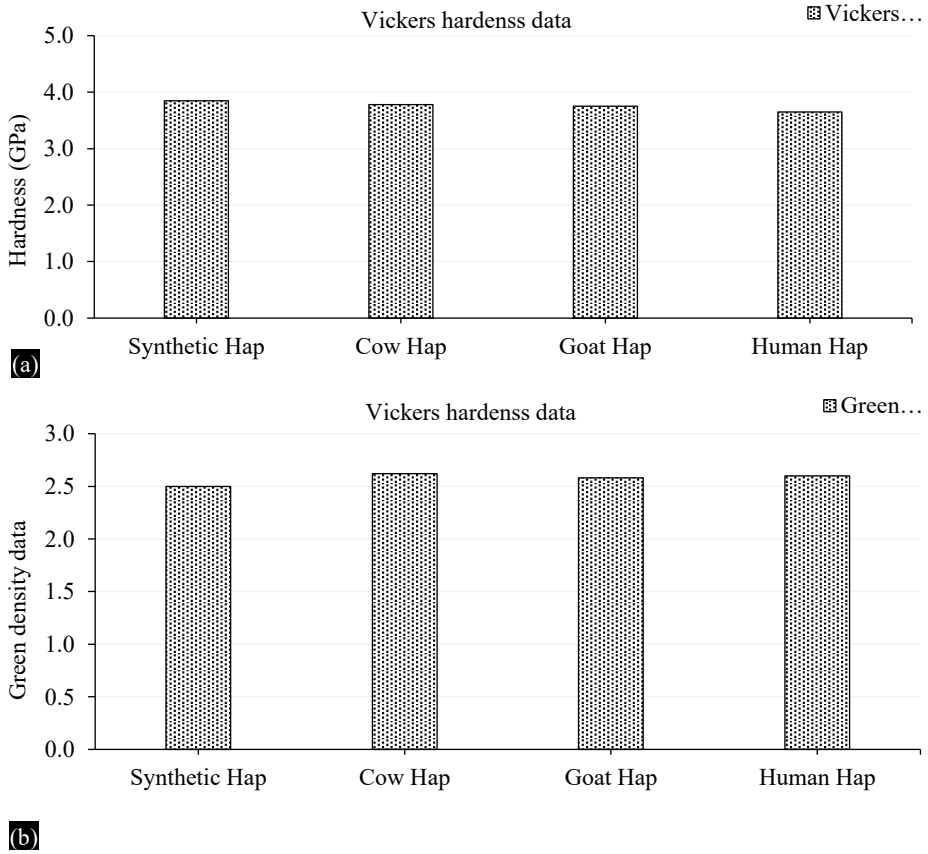

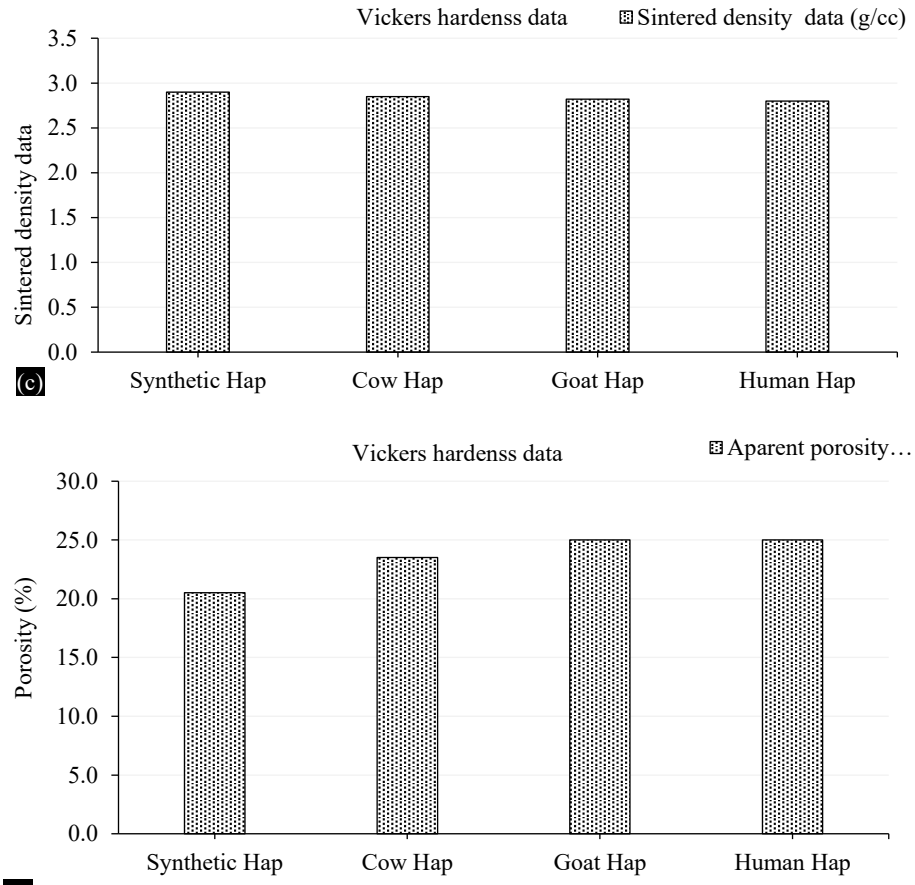

Figure 1. (a)–(d) Diagrammatic representation of the physical properties of hydroxyapatite (HAp) obtained from synthetic and biogenic sources (cow, goat, and human teeth) sintered at 900 °C, showing variations in hardness, green density, sintered density, and apparent porosity.

Although Cow HAp had the highest green density (2.628 g cm^{-3}), the Synthetic HAp achieved the largest densification gain upon sintering. The percent increase from green to sintered density was Synthetic HAp (+16.21%) ,Cow HAp(+8.83%), Goat HAp(+9.01%) and Human HAp (+7.99%).This indicates that the synthetic powder likely possessed higher sintering activity (e.g., due to finer particle size distribution, higher purity, or narrower particle size distribution), which enabled greater densification at 900 °C. In contrast, the biogenic powders densified less under identical conditions—consistent with typical impurity/defect-mediated inhibition of diffusion and neck growth in calcium phosphate ceramics. This reduced densification manifests as higher residual porosity, as evident from below.

To know the relationship between the mechanical response of the hydroxyapatite specimens and their pore construction, a Pearson correlation analysis was performed between the hardness values and the corresponding apparent porosities of the four sample groups. The Pearson correlation coefficient (r) quantifies the degree of linear association between two variables and is calculated using the standard expression:

$$r = \frac{\sum(X_i - \bar{X})(Y_i - \bar{Y})}{\sqrt{\sum(X_i - \bar{X})^2 \sum(Y_i - \bar{Y})^2}}$$

where $X_i$and $Y_i$denote the hardness and porosity measurements, respectively, and $\bar{X}$and $\bar{Y}$represent their mean values.

Table 2. Diametric, linear, and volumetric shrinkage data of specimens during sintering.

Compositions	%Diametric shrinkage	% Linear Shrinkage	% Volumetric Shrinkage
Synthetic HAp	19.20	21.02	47.92
Cow Teeth HAp	19.33	21.23	48.96
Goat Teeth HAp	19.38	21.43	49.25
Human Teeth HAp	19.28	20.95	47.63

Using the experimentally obtained hardness values (3.85, 3.79, 3.76, 3.66 GPa) and porosities (20.74%, 23.53%, 25.29%, 28.97%) for the synthetic, cow-derived, goat-derived, and human-derived HAp samples, a Pearson correlation coefficient of r = –0.996 was obtained. This value, being extremely close to –1, indicates an almost perfect negative linear relationship between hardness and porosity. In practical terms, this implies that as the pore volume increases, the hardness of the material decreases in a highly predictable and linear manner.

This strong negative correlation is consistent with the expected mechanical behavior of porous ceramics. Pores act as microstructural defects that reduce the effective load-bearing area and promote localized stress concentration during indentation. Consequently, materials with higher porosity inherently exhibit lower resistance to deformation. The nearly linear trend observed in the present study indicates that the porosity differences among the four hydroxyapatite sources are the dominant factor governing their hardness response at the sintering temperature of 900 °C.

These findings reaffirm the established understanding that densification and pore elimination play a critical role in enhancing the mechanical integrity of HAp-based biomaterials. Moreover, the close agreement of the experimental data with a near-ideal negative linear trend underscores the reliability of the sample preparation and measurement protocols used in this study.

The porosity values suggest the presence of a substantial void area within the matrix, which is favorable for bone integration. Notably, the human teeth-derived HAp samples exhibit a larger internodular space compared to Synthetic or other derived hydroxyapatite, highlighting their potential advantage in facilitating bone tissue growth and integration. The percentage of porosity is higher in tooth-derived samples, which may be due to their biogenic nature and the huge amount of carbonate present. The percentage of diametric, linear, and volumetric shrinkage of different specimens at sintering temperature of 900 °C is expressed in Table 2.

The shrinkage behavior—diametric, linear, and volumetric—of hydroxyapatite during sintering arises from grain rearrangement, neck growth, pore elimination, and diffusion-driven densification. Shrinkage values (~19–21% linear/diametric and ~47–49% volumetric) are consistent with typical densification ranges for HAp ceramics reported in controlled sintering studies [37]. The small differences between Synthetic, Cow, Goat, and Human HAp reflect slight variations in ion substitution, carbonate levels, crystallinity, and particle morphology, all of which influence shrinkage kinetics. Biogenic HAP (cow, goat, human teeth) naturally contains carbonate and trace elements (e.g., Mg^{2+}, Na^{+}, F^{-}). These influence Crystal lattice distortions. Carbonate-substituted HAP has slightly lower thermal stability and a lower sintering onset temperature, leading to slightly higher shrinkage as reported in some literature. Biogenic HAp typically has finer crystallites and more irregular surfaces, which promote enhanced mass transport and densification, explaining the slightly higher shrinkage in Goat and Cow HAp .

Phase Characterization and Crystal Structure Analysis

The X-ray diffraction (XRD) patterns obtained for hydroxyapatite derived from synthetic, cow-teeth, goat-teeth, and human-teeth sources exhibit well-defined diffraction peaks characteristic of the hexagonal HAp phase. Prominent reflections corresponding to the (002), (211), (202), (300), (212), and (222) crystallographic planes were observed, aligning closely with the standard JCPDS card 09-0432

for stoichiometric hydroxyapatite. The strongest peak located at approximately 2θ ≈ 32.02°, corresponding to the (211) reflection, further supports the formation of a single-phase HAP structure with no detectable secondary calcium phosphate phases.

The XRD profiles (Figure 2) across all samples display highly similar diffraction peak positions and shapes, indicating that theHAp lattice structure remains preserved regardless of biological source. This structural uniformity suggests that the sintering conditions effectively homogenized the microstructure and eliminated most residual organic phases or amorphous components typically present in biogenic apatite.

The lattice parameters are presented in Table 3 below**.**

The regions below 20° and above 50° exhibited negligible diffraction intensities in the uploaded curve, confirming the absence of non-apatitic phases and validating the decision to present only the 20–50° range, where the characteristic HAp peaks are concentrated. This range contains the essential information needed for crystallographic assessment of hydroxyapatite.

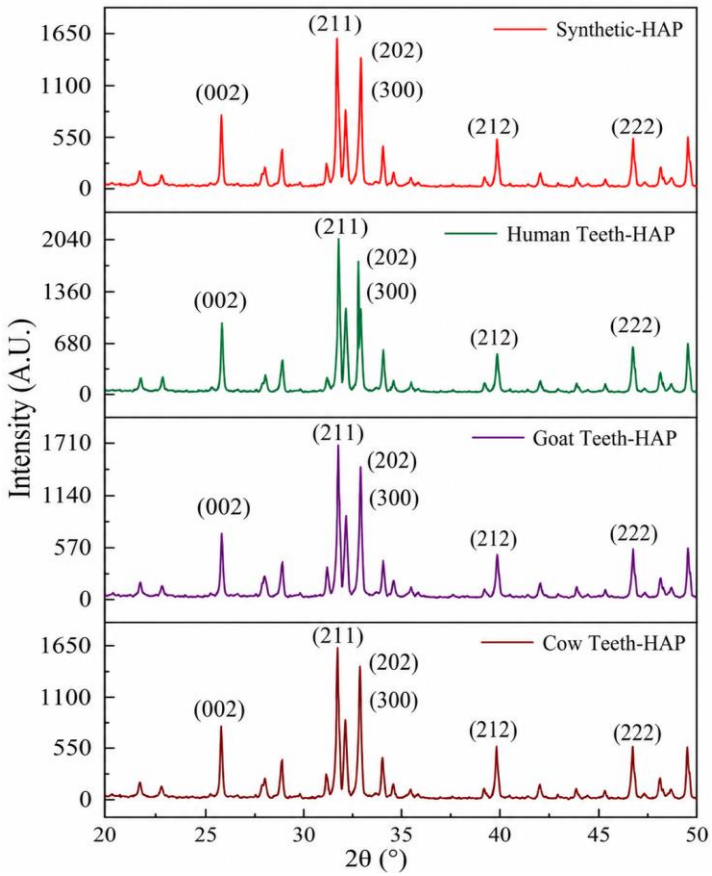

Figure 2. XRD of prepared HAp from different sources. No significant diffraction peaks were observed in the 0–20° and 50–80° ranges; therefore, the data within the 20–50° range are presented**.**

Table 3. Lattice parameters data of tested specimens.

Sample	a axis (Å)	c axis (Å)	Unit cell volume(Å^3)	Crystallite size(Å)	%Crystallinity
Synthetic HAp	9.241±.0.076	6.693 ±0.152	494.98±22.54	3.3681±11.57	82.41± 4.12
CowTeethHAp	9.205±0.33	6.651 ±0.330	488.05±18.29	3.3291±14.77	84.01±5.76
Goat Teeth HAp	9.27±0.35	6.761±0.31	503.15±16.29	3.4121±8.02	82.47±6.82
Human Teeth HAp	9.27±0.22	6.691±0.36	497.94±19.16	3.3912±11.12	88.46±4.02

The calculated lattice parameters (a-axis, c-axis), unit cell volumes, crystallite sizes, and crystallinity percentages (Table 2) showed only minor variations among the samples. Such subtle deviations are expected and can be attributed to ionic substitutions naturally present in biological apatite, including carbonate (CO_3^{2-}), magnesium (Mg^{2+}), sodium (Na^+), and fluoride (F^-). Carbonate substitution is one of the most common chemical modifications in biological hydroxyapatite. Natural bone and teeth contain 4–8 wt% carbonate, incorporated into the HAP crystal lattice during biological mineralization. When HAp is synthesized from biogenic sources (cow, goat, human teeth), this substitution remains even after calcination and sintering, influencing structural, mechanical, and thermal behavior.Carbonate ions (CO_3^{2-}) can replace either the hydroxyl (OH^-) or phosphate (PO_4^{3-}) groups in the HAP lattice.

These substitutions can induce small distortions in the apatite crystal lattice due to differences in ionic radii, leading to the slight expansion or contraction of the a and c lattice parameters observed.

Analysis of Functional Groups

The FTIR spectra of all four samples as shown in Figure 3 display the characteristic phosphate vibrations of hydroxyapatite, including the strong ν_3 band at 1030–1090 cm^{-1}, the sharper ν_1 peak near 960 cm^{-1}, and the ν_4 bending doublet at 560–565 cm^{-1} and 601–605 cm^{-1}, confirming the formation of crystalline stoichiometric HAp in each case. The hydroxyl-related peaks at ~3570 cm^{-1} (stretching) and ~630 cm^{-1} (libration) further indicate that the structural OH^- channels remain intact across all samples, with no evidence of high-temperature decomposition. Weak carbonate bands at 1410–1450 cm^{-1} and ~873 cm^{-1} reveal B-type CO_3^{2-} substitution, more pronounced in the biogenic samples (cow, goat, and human) than in synthetic HAp. Among the four, synthetic HAp shows slightly sharper phosphate and hydroxyl peaks, reflecting higher crystallinity and lower carbonate content, while cow and goat Hap exhibit broader bands due to greater lattice disorder from natural ionic substitutions. Human HAp falls between these extremes, showing moderate carbonate substitution but relatively sharper peaks compared to other biogenic samples, indicating better crystallinity. Overall, the FTIR comparison highlights subtle but consistent differences between synthetic and biogenic HAp, driven mainly by carbonate substitution levels and natural trace-element incorporation.

SEM and EDX Study

SEM images of different samples are shown in Figure 4, which clearly reveal pores, indicating that the prepared samples possess sufficient porosity, which is essential for bone tissue ingrowth.

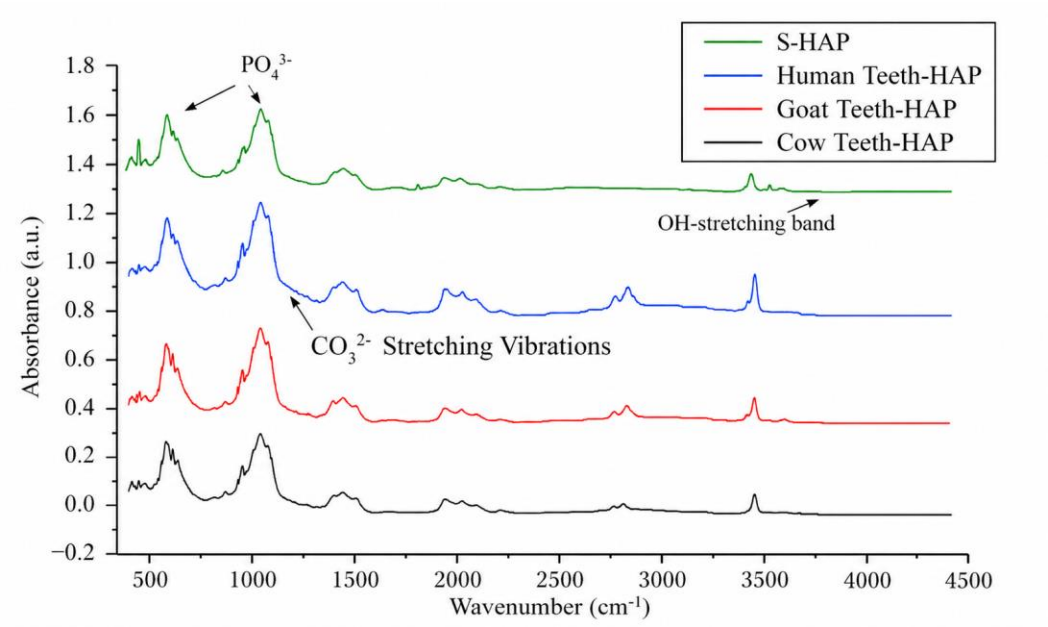

Figure 3. FTIR curve for all samples.

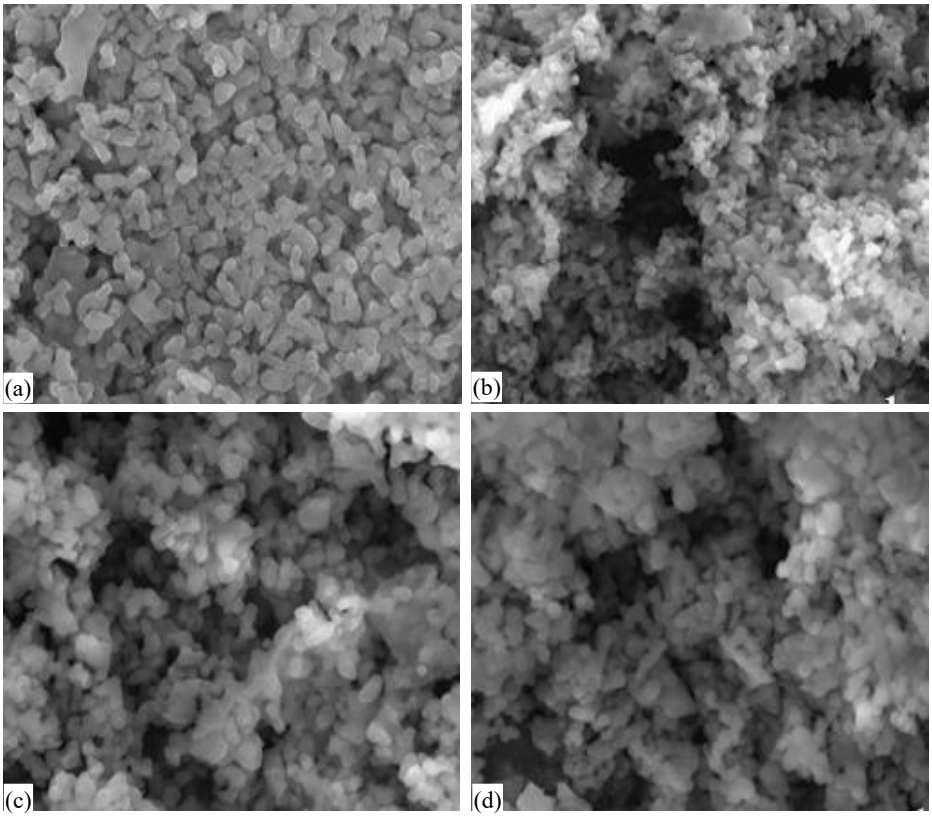

Figure 4. Scanning electron microscopic images: (a)Synthetic HAp (b)CowTeeth derived HAp (c) Goat teeth derived HAp (d) Human teeth derived HAp.

The variation in pore size across the four hydroxyapatite specimens—Synthetic, Cow Teeth, Goat Teeth, and Human Teeth—results from a combination of composition-dependent factors, ionic substitution, powder morphology, and sintering behavior. These factors directly influence densification, grain bonding, and the persistence or collapse of pores during thermal treatment. Biogenic HAps naturally contain carbonate (CO_3^{2-}), Mg^{2+}, Na^{+}, and trace elements, which substitute into the apatite lattice and produce lattice disorder. This disorder lowers the sintering efficiency, resulting in larger and more irregular pores in the Goat and Human samples compared to synthetic HAp. Teeth-derived HAp originates from biological mineral with past organic matrix. Even though calcined, micro-voids from collagen removal can leave larger pore templates that persist after sintering.

BIOLOGICAL CHARACTERIZATION

MTT Assay Analysis

The MTT results are presented in Figure 5 as a bar diagram. It demonstrates that all four hydroxyapatite samples—Synthetic, Cow-derived, Goat-derived, and Human Teeth HAp—exhibited high levels of cell viability, with values consistently close to 100%. This indicates that none of the tested materials induced cytotoxic effects under the experimental conditions. The absorbance values (converted to % viability) suggest that the cells retained normal metabolic activity when exposed to each HAp variant.

Among the groups, Synthetic HAp showed the highest viability, slightly above the 100% control level, suggesting excellent cytocompatibility, likely due to its higher phase purity, lower carbonate substitution, and more uniform microstructure. Cow and Goat Teeth HAp displayed viability very similar to the control, indicating that their biogenic origin and trace ionic substitutions do not negatively impact cell metabolism. Human Teeth HAp also maintained high viability, only marginally lower than the synthetic sample but still well above accepted cytocompatibility thresholds.

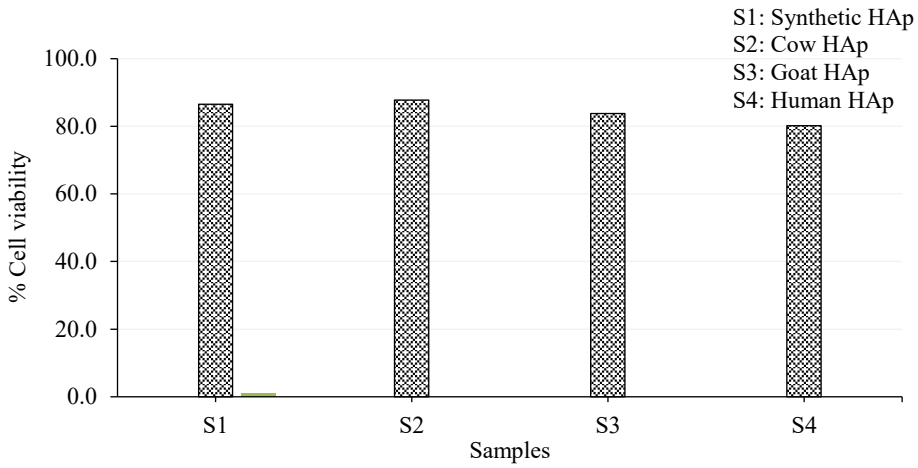

Figure 5. Diagrammatic representation of MTT assay result.

Since MTT viability above 70–80% is considered non-cytotoxic, all four materials clearly meet biocompatibility requirements. The small differences among the samples can be attributed to source-dependent compositional variations (e.g., carbonate content, ionic substitution, and crystallinity), but these variations are not large enough to impair metabolic activity.

Overall, the MTT assay confirms that all prepared HAp powders are cytocompatible, with Synthetic HAp performing slightly better, and the three biogenic HAp showing excellent and comparable cell viability, making them suitable candidates for biomedical applications such as bone regeneration and implant coatings.

Simulated Body Fluid Study

The surface morphology of the samples after immersion in Simulated Body Fluid (SBF) was investigated using Scanning Electron Microscopy (SEM). As shown in Figure 6 (a–d), all samples exhibit the presence of nucleated calcium phosphate (CaP) deposits distributed across the surface (highlighted by red arrows). These precipitates appear as globular or flake-like structures typical of early-stage apatite formation under biomimetic mineralization conditions.

In Sample (a), which corresponds to synthetic hydroxyapatite, the surface shows relatively sparse and loosely bound CaP clusters. The limited quantity of apatite deposition suggests lower bioactivity compared to the biological HAp samples. Synthetic HAp typically lacks the natural trace ions and structural imperfections present in biological apatite, which serve as nucleation accelerators; therefore, its apatite formation rate is inherently lower.

In contrast, Sample (b) derived from cow-bone hydroxyapatite exhibits a significantly denser and more continuous CaP layer. The higher degree of mineral deposition reflects the superior bioactivity of bovine-derived HAp, attributed to its natural carbonate substitution, residual organic components, and crystallinity closer to human bone. These features enhance surface reactivity and strongly promote apatite nucleation in SBF.

Sample (c), representing goat-bone hydroxyapatite, also shows substantial CaP formation, though slightly less pronounced than that of the cow HAp sample. The deposit distribution indicates good bioactivity, yet the nucleation density and aggregate size suggest moderate reactivity relative to bovine HAp. Finally, Sample (d), corresponding to human-derived hydroxyapatite, shows improved CaP formation over synthetic HAp but generally lower than goat and cow HAp. Although chemically similar to natural bone mineral, processing steps such as high-temperature calcination may reduce surface reactivity and diminish available nucleation sites.

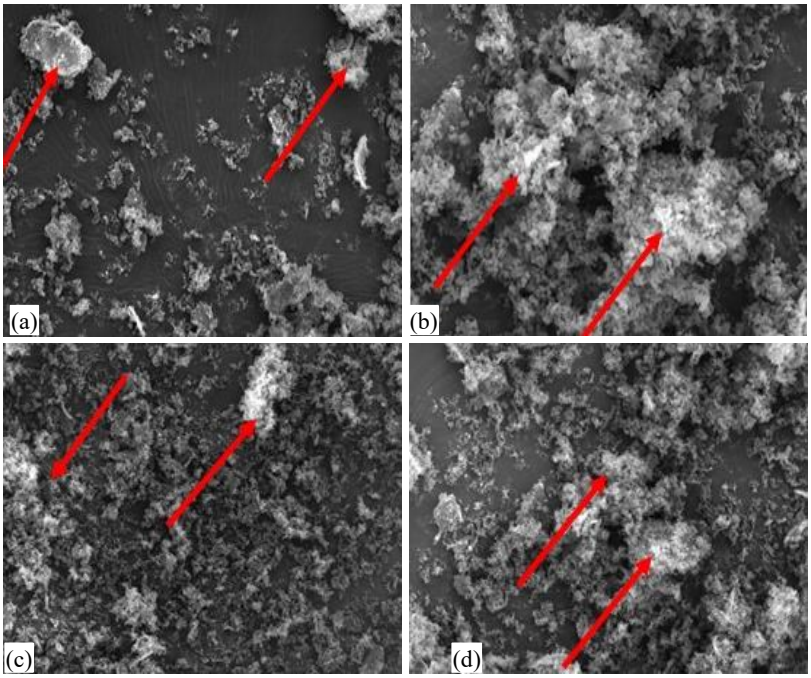

Figure 6. Formation of apatite layers on sintered pellets in SBF solution: (a) Synthetic HAp (b) Cow teeth-derived HAp (c) Goat teeth-derived HAp (d) Human teeth-derived HAp. The red arrow shows the apatite formation area.

Table 4. A set of haemolysis data.

Composition	Wavelength (nm)	Avg. O.D. of Test sample	O.D. (+) ve control	O.D. (-) ve control	% Haemolysis
Synthetic HAp	545	0.069	0.48	0.061	1.90
CowTeethHAp		0.078			4.05
Goat Teeth HAp		0.081			4.52
Human Teeth HAp		0.077			3.81

Haemolysis Study

The hemocompatibility assessment of hydroxyapatite (HAp) derived from different sources revealed that all tested samples exhibited hemolysis percentages below 5%. According to ASTM F756-17, materials with hemolysis values less than 5% are considered highly hemocompatible, thereby confirming the suitability of these samples for biomedical applications involving direct blood contact. This classification is consistent with prior studies that have established hydroxyapatite as a biocompatible and hemocompatible material widely used in bone grafts, coatings, and dental implants. Among the tested compositions, synthetic HAp and cow teeth-derived HAp demonstrated the lowest hemolysis values (1.90% and 4.05%, respectively), indicating superior hemocompatibility compared to goat and human teeth-derived HAp. This observation aligns with reports that synthetic hydroxyapatite, due to its controlled crystallinity and purity, often exhibits enhanced hemocompatibility compared to biologically derived variants. Similarly, cow teeth-derived HAp has been shown to possess favorable physicochemical properties, including high crystallinity and Ca/P ratios close to stoichiometric hydroxyapatite, which contribute to its blood compatibility.The slightly higher hemolysis percentages observed in goat (4.52%) and human teeth-derived HAp (3.81%) may be attributed to variations in mineral content, crystallinity, and trace organic residues inherent to biological sources. Previous studies have noted that such compositional differences can influence surface interactions with erythrocytes, thereby affecting hemolysis outcomes. Nevertheless, these values remain well within the ASTM threshold, confirming their safety for biomedical use. Among the different compositions, pure HAp and Cow teeth HAp have shown the maximum haemocompatibility. A set of haemolysis data is presented in Table 4 below.

CONCLUSION

This study demonstrates that human and cattle dental waste represent viable, sustainable, and efficient raw materials for the production of biogenic hydroxyapatite suitable for biomedical applications. Comprehensive physicochemical analyses—including XRD, FTIR, SEM, hardness testing, and porosity assessment—confirmed that HAp derived from human, cow, and goat teeth exhibits structural and functional characteristics comparable to conventional laboratory-synthesized HAp. All biogenic samples displayed well-defined apatite crystal phases, characteristic phosphate and hydroxyl functional groups, and microstructures conducive to osteoconductivity. Minor variations observed in lattice parameters, crystallinity, and functional group intensities were attributed primarily to natural ionic substitutions such as carbonate, magnesium, sodium, and fluoride inherent to biological sources. Mechanical characterization revealed consistent hardness, densification behavior, and shrinkage patterns across all samples, with a nearly perfect negative correlation ($r = –0.996$) between porosity and hardness, affirming that pore architecture strongly governs mechanical performance. The higher porosity observed in biogenic HAp, particularly human teeth-derived samples, may be advantageous for bone ingrowth, nutrient diffusion, and vascularization in implant applications. Biological assays further established the biomedical safety of all samples. MTT viability values remained near or above 100%, confirming excellent cytocompatibility and absence of cytotoxic effects. Hemolysis percentages for all compositions were below the ASTM F756-17 threshold of 5%, classifying them as highly hemocompatible. Importantly, SBF immersion studies revealed enhanced apatite nucleation in biogenic HAp compared to synthetic HAp, underscoring their superior bioactivity—largely influenced by natural trace ions and microstructural irregularities that promote surface reactivity. The findings validate the concept of converting human and cattle dental waste into high-quality, functional hydroxyapatite biomaterials with strong potential for use in bone regeneration, implant coatings, and other clinical applications.

Conflicts of Interest

The authors declare that they have no conflicts of interest

Acknowledgements

The authors wish to acknowledge the Department of Biomedical Engineering for extending help in performing all laboratory work.

Author Contribution

The first and second authors contributed equally to this work and share first authorship.

REFERENCES

1. K. Manickaraj et al., “Value-added utilization of agricultural wastes in biocomposite production: Characteristics and applications,” Jul. 01, 2025, John Wiley and Sons Inc. doi: 10.1111/nyas.15368.
2. A. K. S. P. and N. A. Rajkumar Ramasubbu, “Mechanical Properties of Epoxy Composites Reinforced with Areca catechu Fibers Containing Silicon Carbide,” Bioresources, no. 2, pp. 2353–2370, 2024, doi: DOI:10.15376/biores.19.2.2353-2370.
3. S. Palanisamy et al., “Effects of fiber loadings and lengths on mechanical properties of Sansevieria Cylindrica fiber reinforced natural rubber biocomposites,” Mater. Res. Express, vol. 10, no. 8, Aug. 2023, doi: 10.1088/2053-1591/acefb0.
4. N. Ayrilmis, G. Kanat, E. Yildiz Avsar, S. Palanisamy, and A. Ashori, “Utilizing waste manhole covers and fibreboard as reinforcing fillers for thermoplastic composites,” Journal of Reinforced Plastics and Composites, vol. 44, no. 17–18, pp. 1108–1118, Sep. 2025, doi: 10.1177/07316844241238507.
5. S. P. T. mani M. S. T. R. K. S. A. and C. S. e Murugesan Palaniappan, “Influence of Washing with Sodium Lauryl Sulphate (SLS) Surfactant on Different Properties of Ramie Fibres,” Bioresources, no. 19 (2), pp. 2609–2625, doi: DOI:10.15376/biores.19.2.2609-2625.
6. B. Mylsamy, K. Aruchamy, S. K. Marudhamuthu Shanmugam, S. Palanisamy, and N. Ayrılmis, “Improving performance of composites: Natural and synthetic fibre hybridisation techniques in

composite materials – A review," Apr. 01, 2025, Elsevier Ltd. doi: 10.1016/j.matchemphys.2025.130439.
7. H. Boukhris, H. Zidani, A. B. H. Khalifa, G. Bouslema, and S. B. Youssef, "Environmental Impact of Dental Waste: A Survey-based Analysis of Waste Segregation and Recycling Practices in Dental Clinics," Journal of Contemporary Dental Practice, vol. 26, no. 3, pp. 250–256, 2025, doi: 10.5005/jp-journals-10024-3845.
8. E. Klimuszko, K. Orywal, T. Sierpinska, J. Sidun, and M. Golebiewska, "Evaluation of calcium and magnesium contents in tooth enamel without any pathological changes: in vitro preliminary study," Odontology, vol. 106, no. 4, pp. 369–376, Oct. 2018, doi: 10.1007/s10266-018-0353-6.
9. J. T. B. Ratnayake, M. Mucalo, and G. J. Dias, "Substituted hydroxyapatites for bone regeneration: A review of current trends," J. Biomed. Mater. Res. B Appl. Biomater., vol. 105, no. 5, pp. 1285–1299, Jul. 2017, doi: 10.1002/jbm.b.33651.
10. G. Tripathi and B. Basu, "A porous hydroxyapatite scaffold for bone tissue engineering: Physico-mechanical and biological evaluations," Ceram. Int., vol. 38, no. 1, pp. 341–349, Jan. 2012, doi: 10.1016/j.ceramint.2011.07.012.
11. F. B. Bagambisa and U. Joos, "Preliminary studies on the phenomenological behaviour of osteoblasts cultured on hydroxyapatite ceramics," Biomaterials, vol. 11, no. 1, pp. 50–56, Jan. 1990, doi: 10.1016/0142-9612(90)90052-R.
12. P. R. Dev, C. P. Anand, D. S. Michael, and P. Wilson, "Hydroxyapatite coatings: a critical review on electrodeposition parametric variations influencing crystal facet orientation towards enhanced electrochemical sensing," Sep. 06, 2022, Royal Society of Chemistry. doi: 10.1039/d2ma00620k.
13. T. Hoai, N. K. Nga, G. Luu Truong, T. Huy, T. Phan Nguyen, and B. Binh, "Hydrothermal Synthesis of Hydroxyapatite Nanorods for Rapid Formation of Bone-Like Mineralization," J. Electron. Mater., vol. 46, Apr. 2017, doi: 10.1007/s11664-017-5509-6.
14. Y. Chang-Chen et al., "Hydrothermal synthesis of hydroxyapatite nanoparticles using biosurfactant and application on mesenchymal stem cells," Ceram. Int., vol. 51, Feb. 2025, doi: 10.1016/j.ceramint.2025.02.088.
15. G. Guo, Y. Wang, Z. Wang, and H. Guo, "Study on the synthesis of hydroxyapatite nanoparticles by the chemical precipitation method," vol. 67, pp. 830–834, Jan. 2004.
16. I. Sopyan, R. Singh, and M. Abd Shukor, "Synthesis of nano sized hydroxyapatite powder using sol-gel technique and its conversion to dense and porous bodies," Indian Journal of Chemistry Section a, vol. 47, pp. 1626–1631, Nov. 2008.
17. S. Jarudilokkul, W. Tanthapanichakoon, and V. Boonamnuayvittaya, "Synthesis of hydroxyapatite nanoparticles using an emulsion liquid membrane system," Colloids Surf. A Physicochem. Eng. Asp., vol. 296, pp. 149–153, Mar. 2007, doi: 10.1016/j.colsurfa.2006.09.038.
18. I. Kimura, "Synthesis of Hydroxyapatite by Interfacial Reaction in a Multiple Emulsion," Research Letters in Materials Science, vol. 2007, pp. 1–4, 2007, doi: 10.1155/2007/71284.
19. M. S. Baltatu, A. V. Sandu, M. Nabialek, P. Vizureanu, and G. Ciobanu, "Biomimetic deposition of hydroxyapatite layer on titanium alloys," Micromachines (Basel)., vol. 12, no. 12, Dec. 2021, doi: 10.3390/mi12121447.
20. F. L. Muntean et al., "Hydroxyapatite from Mollusk Shells: Characteristics, Production, and Potential Applications in Dentistry," Dec. 01, 2024, Multidisciplinary Digital Publishing Institute (MDPI). doi: 10.3390/dj12120409.
21. M. Saravanan, S. Krishnamoorthi, N. Rajaram, and M. Saravanakumar, "Synthesis of Nano-Hydroxyapatite from Sea Shell and Squid Bone Waste for Advanced Bone Applications via Precipitation Process," SSRG International Journal of Mechanical Engineering, vol. 12, no. 9, pp. 130–138, Sep. 2025, doi: 10.14445/23488360/IJME-V12I9P113.
22. C. Y. Ooi, M. Hamdi, and S. Ramesh, "Properties of hydroxyapatite produced by annealing of bovine bone," Ceram. Int., vol. 33, no. 7, pp. 1171–1177, Sep. 2007, doi: 10.1016/j.ceramint.2006.04.001.

23. S. Joschek, B. Nies, R. Krotz, and A. Göpferich, "Chemical and physicochemical characterization of porous hydroxyapatite ceramics made of natural bone," Biomaterials, vol. 21, no. 16, pp. 1645–1658, Aug. 2000, doi: 10.1016/S0142-9612(00)00036-3.
24. C. Balázsi, F. Wéber, Z. Kövér, E. Horváth, and C. Németh, "Preparation of calcium-phosphate bioceramics from natural resources," J. Eur. Ceram. Soc., vol. 27, no. 2–3, pp. 1601–1606, 2007, doi: 10.1016/j.jeurceramsoc.2006.04.016.
25. G. Gergely et al., "Preparation and characterization of hydroxyapatite from eggshell," Ceram. Int., vol. 36, pp. 803–806, Mar. 2010, doi: 10.1016/j.ceramint.2009.09.020.
26. J. Rocha et al., "Scaffolds for Bone Restoration From Cuttlefish," Bone, vol. 37, pp. 850–857, Jan. 2006, doi: 10.1016/j.bone.2005.06.018.
27. H. L. Jaber, A. S. Hammood, and N. Parvin, "Synthesis and characterization of hydroxyapatite powder from natural Camelus bone," Journal of the Australian Ceramic Society, vol. 54, no. 1, pp. 1–10, Mar. 2018, doi: 10.1007/s41779-017-0120-0.
28. Y. Z. Wan et al., "Synthesis and characterization of hydroxyapatite–bacterial cellulose nanocomposites," Compos. Sci. Technol., vol. 66, no. 11–12, pp. 1825–1832, Sep. 2006, doi: 10.1016/j.compscitech.2005.11.027.
29. A. Ruksudjarit, K. Pengpat, G. Rujijanagul, and T. Tunkasiri, "Synthesis and characterization of nanocrystalline hydroxyapatite from natural bovine bone," Current Applied Physics, vol. 8, no. 3–4, pp. 270–272, May 2008, doi: 10.1016/j.cap.2007.10.076.
30. D. & S. S. & D. S. & R. S. & B. P. & N. Samit. Acharjee, "Journal of mines metals and fuels," Journal of Mines, Metals and Fuels, vol. 71, no. 11, pp. 1–8, Dec. 2023, Accessed: Sep. 01, 2024. [Online]. Available: DOI: https://doi.org/10.18311/jmmf/2023/33731
31. S. K. Samanta and A. Chanda, "Study on different characteristics of doped tri calcium phosphate at different sintering temperatures," in AIP Conference Proceedings, American Institute of Physics Inc., Apr. 2016. doi: 10.1063/1.4945162.
32. T. Kokubo and H. Takadama, "How useful is SBF in predicting in vivo bone bioactivity?," Biomaterials, vol. 27, no. 15, pp. 2907–2915, 2006, doi: 10.1016/j.biomaterials.2006.01.017.
33. T. Kokubo, H. Kushitani, S. Sakka, T. Kitsugi, and T. Yamamuro, "Solutions able to reproduce in vivo surface-structure changes in bioactive glass-ceramic A-W3," J. Biomed. Mater. Res., vol. 24, no. 6, pp. 721–734, 1990, doi: 10.1002/jbm.820240607.
34. M. Hoffman and D. M. Monroe, "Coagulation 2006: a modern viewof hemostasis. Hematology/Oncol," Clin. North Am., vol. 21, pp. 1–11, 2007.
35. P. Bhattacharjee, H. Begam, A. Chanda, and S. K. Nandi, "Animal trial on zinc doped hydroxyapatite: A case study," Journal of Asian Ceramic Societies, vol. 2, no. 1, pp. 44–51, 2014, doi: 10.1016/j.jascer.2014.01.005.
36. D. Acharjee, S. Debnath, P. Basak, S. Roy, and S. Kumar Nandi, "IN-VITRO CHARACTERISATION OF MAGNESIUM DOPED HYDROXYAPATITE DEVELOPED FROM CALCIUM HYDROXIDE AND WASTE EGGSHELL."
37. K. I. Sokol and R. V Vovk, "Functional characteristics of hydroxyapatite sintered at high temperatures," Vovk Journal of V. N. Karazìn Kharkiv National University. Series Physics. Iss, vol. 39, p. 2023, 2023, doi: 10.26565/2222-5617-2023-39.

